ISSN 1070-3284, Russian Journal of Coordination Chemistry, 2009, Vol. 35, No. 7, pp. 541–546. © Pleiades Publishing, Ltd., 2009.

Synthesis, Structure, and Antibacterial Properties of Ternary Rare-Earth Complexes with *o*-Methylbenzoic Acid and 1,10-Phenanthroline[1]

Z. M. Chen[a], S. P. Wang[a], N. Yang[c], N. Zhao[a], J. J. Zhang[b], R. F. Wang[a]*, and B. H. Zhao[c]
[a] *College of Chemistry & Material Science, Hebei Normal University, Shijiazhuang, 050016 P. R. China*
[b] *Experimental Center, Hebei Normal University, Shijiazhuang, 050016 P. R. China*
[c] *College of Life Science, Hebei Normal University, Shijiazhuang, 050016 P. R. China*
**E-mail: wruifen@mail.hebtu.edu.cn*

Received October 14, 2008

Abstract—Ternary rare-earth complexes with *o*-methylbenzoic acid (*o*-MBA) and 1,10-phenanthroline (Phen) $Ln_2(o\text{-MBA})_6(Phen)_2 \cdot nH_2O$ ($n = 0$, 1) (Ln = La, Pr, Y, Yb) were synthesized and characterized by elemental analysis, IR, X-ray diffraction, and TG-DTG means. The complex $La_2(o\text{-MBA})_6$ $(Phen)_2 \cdot H_2O$ (**I**) is composed of two species of binuclear molecules in which the La^{3+} ion is coordinated with two nitrogen atoms of Phen and seven oxygen atoms of carboxylate groups. The carboxylate groups were bonded to La^{3+} in three modes: chelating-bidentate, bridging-bidentate, and chelating-bridging tridentate. The La^{3+} ion adopted a vigorous distorted monocapped square antiprism geometry. Complex **I** belongs to the triclinic crystal system, $P\bar{1}$ space group, lattice parameters: a = 13.058(3), b = 12.7584(11), c = 20.773(4) Å, α = 101.18(3)°, β = 93.88(3)°, γ = 115.82(3)°, V = 3283.0(11)Å^3, Z = 2, ρ_{calcd} = 1.484 mg/m^3, M_r = 1467.06, $F(000)$ = 1476, μ = 1.350 mm^{-1}. The structure was refined to R_1 = 0.0631 and wR_2 = 0.1504. The antibacterial activity test indicates that these complexes exhibit better antibacterial ability against *Escherichia coli* and *Staphylococcus aureus* than the corresponding rare–earth chloride or *o*-MBA.

DOI: 10.1134/S1070328409070124

INTRODUCTION

It is well known that almost all metals enable to generate reactive oxygen species, and this property is mainly used for the treatment of cancer and other diseases. Some rare-earth ions may participate in various physicochemical processes of living systems. They also show efficient inhibitory properties for $O_2^{-\bullet}$ and $OH^{\bullet}$ [1, 2]. So, they exhibit good functions as antibacterial and antiphlogistic compounds [3–5].

In the last decades, research of rare-earth organic materials has been a very attractive subject due to their peculiar properties and wide potential applications as luminescence probes in biological systems and active centers for luminescent materials or electroluminescent devices [6–8]. In particular, their peculiar functions in life science and clinical medicine have attracted people's great interests [9–11]. For instance, they can be used as diagnostic imaging agents, antibacterial and antiphlogistic agents, etc [4, 5, 12]. In this paper, a series of complexes containing Ln^{3+} (Ln = La (**I**), Pr (**II**), Y (**III**), Yb (**IV**)), *o*-methylbenzoic acid (***o*-MBA**) and 1.10-phenanthroline (**Phen**), $Ln_2(o\text{-MBA})_6(Phen)_2 \cdot nH_2O$ (n = 0, 1), were synthesized and characterized, and their antibacterial activities were investigated in detail.

EXPERIMENTAL

Ln_2O_3 (Ln = La, Pr, Y, Yb), (*o*-MBA), and Phen were purchased. All reagents were analytical grade and used without further purification. $LnCl_3 \cdot 6H_2O$ were prepared by reacting their oxides in hydrochloric acid, and then the solutions were dried by water-bath heating.

The contents of C, H, and N in the complexes **I–IV** were measured by a Flash EA 1112 elemental analyzer. The FT-IR spectra were recorded on a FT-IR 1730 spectrometer in the 3500–350 cm^{-1} region, using KBr pellets. The single-crystal was determined on a Bruker XSCANS P4 diffractometer equipped with a graphite monochromated MoK_α radiation.

The antibaterial activity was tested by the disc diffusion method using the Mueller-Hinton agar medium. Sterile filter paper discs (5 cm in diameter) were soaked in 20 µl solutions prepared in sterile DMF. Five concentrations of the test compounds, viz., 0.004, 0.006, 0.008,

---

[1] The article is published in the original.

Table 1. Analytical data for the complexes $Ln_2(o\text{-MBA})_6(Phen)_2 \cdot nH_2O$

Compound	Empirical formula	Contents (found/calcd), %		
		C	H	N
I	$C_{72}H_{60}O_{13}N_4La_2$	59.49/58.95	4.15/4.12	3.92/3.82
II	$C_{36}H_{29}O_6N_2Pr$	59.51/59.02	4.02/4.32	3.86/3.89
III	$C_{36}H_{29}O_6N_2Y$	64.10/63.73	4.33/4.76	4.15/4.14
IV	$C_{36}H_{29}O_6N_2Yb$	56.99/56.54	3.85/3.89	3.69/3.71

Table 2. Crystallographic data and details of the experiment and refinement of structure **I**

Parameter	Value
Formula weight	1467.06
Crystal system	Triclinic
Space group	$P\bar{1}$
Unit cell dimensions:	
a, Å	13.058 (3)
b, Å	12.7584 (11)
c, Å	20.773 (4)
α, deg	101.18 (3)
β, deg	93.88 (3)
γ, deg	115.82 (3)
V, Å^3	3283.0 (11)
Z	2
ρ_{calcd}, mg/m^3	1.484
Absorption coefficient mm^{-1}	1.350
F(000)	1476
Crystal size, mm	0.22 × 0.15 × 0.12
θ range for data collection, deg	1.68–25.00
Index ranges	$-15 \le h \le 15$ $-11 \le k \le 16$ $-24 \le l \le 18$
Reflections collected/unique	16755/11552 (R_{int} = 0.0491)
Completeness to θ = 28.27°, %	97.6
Absorption correction	Empirical
Max and min transmission	0.850 and 0.784
Data/restraints/parameters	11277/0/834
Goodness-of-fit on F^2	1.036
Final R indices ($I > 2\sigma(I)$)	$R_1 = 0.0631$ $wR_2 = 0.1504$
R indices (all data)	$R_1 = 0.1075$ $wR_2 = 0.1836$
Largest diff. peak and hole, e Å^{-3}	2.344 and –1.454

0.010, and 0.012 mol l^{-1}, were prepared and tested against *Escherichia coli* and *Staphylococcus aureus*. The bacterial concentration was $OD_{600} = 1$. The antibacterial effects were investigated after 18–24 h of incubation at 37°C. The antibacterial activity was classifed as highly active (diameter (dia) ≥ 15 mm), moderately active (dia = 10–15 mm), and slightly active (dia = 5–10 mm). The diameter less than 5 mm was regarded as inactive [13].

Synthesis of rare-earth complexes. An ethanol solution containing *o*-MBA (6.0 mmol) and Phen (2.0 mmol) was adjusted to pH 6.0–7.0 with a 1.0 mol l^{-1} NaOH solution and then was added dropwise to the stirred aqueous solution of $LnCl_3$ (2.0 mmol), while a white precipitate formed (Pr(III) complex is light green). The mixture was stirred for 5 h at room temperature, filtered, and dried. The mother liquor was evaporated at room temperature, and a colorless transparent crystal suitable for X-ray analysis was obtained from the mother liquor of La(III).

All four complexes **I–IV** were synthesized by this method. The molecular composition of four complexes is shown in the Table 1.

X-ray crystallographic determination. A colorless single crystal of complex **I** was put on a Bruker XSCANS P4 diffractometer equipped with a graphite monochromated MoK_α radiation (λ = 0.71073 Å) at 293(2) K by using an ω scans technique. The usual *Lp* and empirical absorption corrections were applied by the SADABS program. The structures were solved by direct methods with SHELXS-97 [14] and refined using a full-matrix least-squares procedure on F^2 in SHELXL-97 [15]. Hydrogen atoms were added theoretically and refined with riding model position parameters and fixed isotropic thermal parameters. The final $R = 0.0631$, $wR = 0.1504$ ($R = \Sigma(||F_o| - |F_c||)/|F_o|$, $wR = (\Sigma w(|F_o|^2 - |F_c|^2)^2/\Sigma w|F_o|^2)^{1/2}$, $w = 1/[\sigma^2(F_o^2) + (0.0295P)^2 + 0.6213P]$, where $P = (F_o^2 + 2F_c^2)/3$), $S = 1.050$, $(\Delta\rho)_{max} = 2.344$, $(\Delta\rho)_{min} = -1.454$ e Å^{-3}, and (Δ/σ)max = 0.026. Crystallographic data and experimental details for structural analyses are summarized in Table 2.

Supplementary material has been deposited with the Cambridge Crystallographic Data Centre (no. 705097; deposit@ccdc.cam.ac.uk or www:http://www.ccdc.cam.ac.uk).

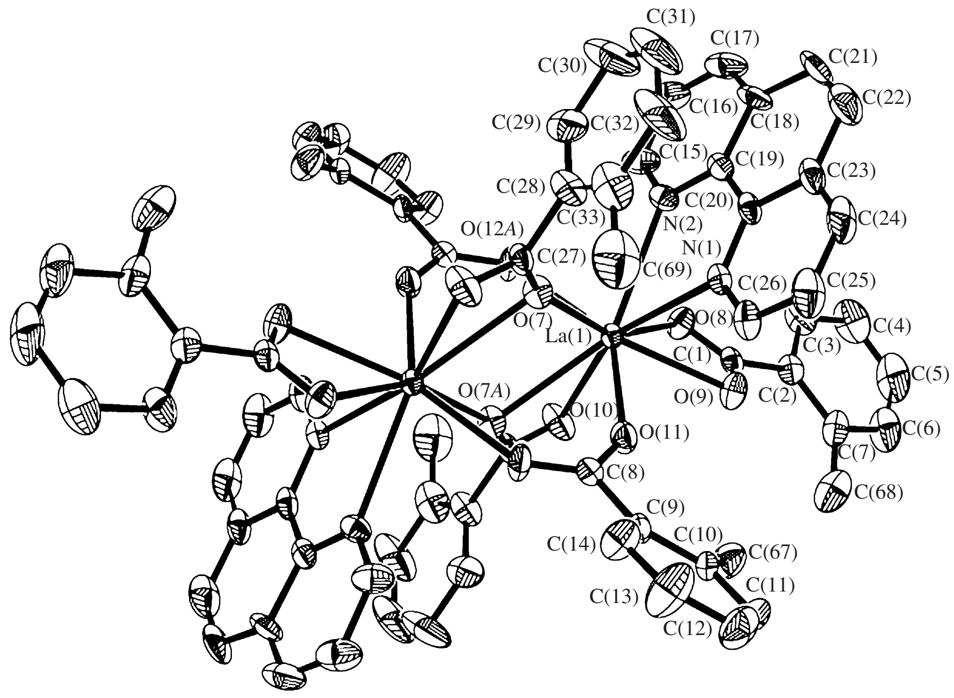

Fig. 1. ORTEP drawing of the dimeric structure for complex **I**, La(1).

The TG-DTG curves of the four complexes in a static air atmosphere are performed on a Perkin-Elmer TGA-7 thermogravimetric analyzer from room temperature to 930°C with a heating rate of 10°C min^{-1}.

RESULTS AND DISCUSSION

Compared with the IR spectra of *o*-MBA and Phen · H_2O, the characteristic peaks of the ligands have obviousely shifts in all spectra of complexes **I–IV**. The characteristic absorption of ν(C=O) (1690 cm^{-1}) in *o*-MBA disappeared completely while ν_{as} (1609–1639 cm^{-1}) and ν_s (1400–1410 cm^{-1}) of the carboxyl group appeared, suggesting that the carboxyl group was coordinated to Ln^{3+} ions [16, 17]. In addition, the absorption band of ν(C=N) (1560 cm^{-1}) in Phen shifts to 1518 cm^{-1} in the spectra of the complexes, exhibiting the coordination of the two nitrogen atoms with Ln^{3+} ion [18]. Furthermore, the broad peak around 3447 cm^{-1} is ascribed to the stretching vibration of the crystal water molecule [19]. The peak of 475 cm^{-1} was assigned to ν(Ln–O), further testifying that the oxygens of the carboxyl group coordinate to Ln^{3+} ions [20, 21].

The crystal of complex **I** contains two independent dimeric molecules $La_2(o\text{-MBA})_6(\text{Phen})_2 \cdot H_2O$, noted as La(1) and La(2), respectively. The structure for La(1) is shown in Fig. 1. Selected bond lengths and angles are listed in Table 3. La(1) and La(2) are identical in composition with similar structures. In each molecule, two Ln^{3+} ions are linked by four bridging carboxylate groups forming a dimer with a crystallographic inversion center. Two of the bridging *o*-MBA adopt the bidentate bridging mode, the other two *o*-MBA adopt the tridentate bridging mode. Each Ln^{3+} ion is coordinated to nine atoms, of which two oxygen atoms O(11), O(12*A*) are from the bidentate chelating carboxylate, two oxygen atoms O(8), O(9) from two bidentate bridging carboxylates, three oxygen atoms O(7), O(7A), O(10) from two tridentate bridging chelating carboxylates, and two nitrogen atoms N(1), N(2) from a Phen molecule. The five-membered chelate ring containing two nitrogen atoms and the Ln^{3+} ion are coplanar to the Phen plane. In La(1), the distance between two Ln^{3+} ions is 4.117 Å, the average La–O bond length is 2.545 Å, the average La–N bond length is 2.733 Å. In La(2), the distance between two Ln^{3+} ions is 2.733 Å, the mean La–O bond length is 2.550 Å, the average La–N bond length is 2.733 Å, which is equal to that of La(1). These data indicate that the interaction between the Ln^{3+} ions and oxygen atoms in La(1) is stronger than in La(2), but the interactions between the La^{3+} ions and nitrogen atoms are identical in La(1) and La(2).

The central Ln^{3+} adopts vigorous distorted monocapped square antiprism in both La(1) and La(2) (Fig. 2). In La(1), the cap position is occupied by N(1) (the longest bond in the polyhedron of La^{3+}). The four positions of the upper square are occupied by O(7), O(9), O(11), N(2), the lower square is formed by O(8), O(10), O(7*A*), O(12*A*). In La(2), the cap position is occupied by N(4) (the longest bond in polyhedron of La^{3+}). The four positions of the upper square are occupied by O(2), O(5), O(6), and N(3), and the lower square is formed by O(1), O(3), O(4), and O(6*A*).

Table 3. Bond lengths and bond angles for complex **I***

Bond	d, Å	Bond	d, Å
La(1)–O(11)	2.446(6)	La(2)–O(5)	2.455(6)
La(1)–O(7)	2.476(5)	La(2)–O(4)	2.476(6)
La(1)–O(12)$^{\#1}$	2.487(6)	La(2)–O(6)	2.489(6)
La(1)–O(9)	2.558(6)	La(2)–O(1)	2.536(6)
La(1)–O(8)	2.577(6)	La(2)–O(2)	2.549(6)
La(1)–O(10)	2.594(6)	La(2)–O(3)	2.610(6)
La(1)–O(7)$^{\#1}$	2.689(6)	La(2)–N(3)	2.706(7)
La(1)–N(2)	2.712(8)	La(2)–O(6)$^{\#2}$	2.734(6)
La(1)–N(1)	2.753(7)	La(2)–N(4)	2.760(7)
Angle	ω, deg	Angle	ω, deg
O(11)La(1)O(7)	73.9(2)	O(5)La(2)O(4)	134.12(18)
O(11)La(1)O(12)$^{\#1}$	134.4(2)	O(5)La(2)O(6)	73.46(19)
O(7)La(1)O(12)$^{\#1}$	74.0(2)	O(4)La(2)O(6)	75.38(19)
O(11)La(1)O(9)	79.8(2)	O(5)La(2)O(1)	141.7(2)
O(7)La(1)O(9)	142.4(2)	O(4)La(2)O(1)	73.6(2)
O(12)$^{\#1}$La(1)O(9)	141.8(2)	O(6)La(2)O(1)	144.7(2)
O(11)La(1)O(8)	127.4(2)	O(5)La(2)O(2)	96.92(19)
O(7)La(1)O(8)	156.7(2)	O(4)La(2)O(2)	125.08(19)
O(12)$^{\#1}$La(1)O(8)	92.0(2)	O(6)La(2)O(2)	152.3(2)
O(9)La(1)O(8)	50.0(2)	O(1)La(2)O(2)	51.6(2)
O(11)La(1)O(10)	92.1(3)	O(5)La(2)O(3)	72.37(19)
O(7)La(1)O(10)	122.1(2)	O(4)La(2)O(3)	96.7(2)
O(12)$^{\#1}$La(1)O(10)	78.5(3)	O(6)La(2)O(3)	121.00(18)
O(9)La(1)O(10)	84.7(2)	O(1)La(2)O(3)	79.4(2)
O(8)La(1)O(10)	71.3(2)	O(2)La(2)O(3)	78.42(19)
O(11)La(1)O(7)$^{\#1}$	67.7(2)	O(5)La(2)N(3)	130.7(2)
O(7)La(1)O(7)$^{\#1}$	74.4(2)	O(4)La(2)N(3)	77.0(2)
O(12)$^{\#1}$La(1)O(7)$^{\#1}$	73.0(2)	O(6)La(2)N(3)	83.5(2)
O(9)La(1)O(7)$^{\#1}$	119.3(2)	O(1)La(2)N(3)	73.4(2)
O(8)La(1)O(7)$^{\#1}$	119.9(2)	O(2)La(2)N(3)	83.7(2)
O(10)La(1)O(7)$^{\#1}$	48.94(19)	O(3)La(2)N(3)	152.7(2)
O(11)La(1)N(2)	135.9(2)	O(5)La(2)O(6)$^{\#2}$	71.39(18)
O(7)La(1)N(2)	88.8(2)	O(4)La(2)O(6)$^{\#2}$	68.66(19)
O(12)$^{\#1}$La(1)N(2)	74.3(2)	O(6)La(2)O(6)$^{\#2}$	75.24(19)
O(9)La(1)N(2)	91.9(2)	O(1)La(2)O(6)$^{\#2}$	108.15(18)
O(8)La(1)N(2)	69.2(2)	O(2)La(2)O(6)$^{\#2}$	127.22(19)
O(10)La(1)N(2)	130.5(2)	O(3)La(2)O(6)$^{\#2}$	48.83(17)
O(7)$^{\#1}$La(1)N(2)	146.2(2)	N(3)La(2)O(6)$^{\#2}$	143.1(2)
O(11)La(1)N(1)	76.3(2)	O(5)La(2)N(4)	73.3(2)
O(7)La(1)N(1)	74.3(2)	O(4)La(2)N(4)	131.1(2)
O(12)$^{\#1}$La(1)N(1)	123.7(2)	O(6)La(2)N(4)	78.4(2)
O(9)La(1)N(1)	73.8(2)	O(1)La(2)N(4)	110.3(2)
O(8)La(1)N(1)	99.7(2)	O(2)La(2)N(4)	73.8(2)
O(10)La(1)N(1)	157.0(2)	O(3)La(2)N(4)	132.2(2)
O(7)$^{\#1}$La(1)N(1)	137.4(2)	N(3)La(2)N(4)	59.5(2)
N(2)La(1)N(1)	59.8(2)	O(6)$^{\#2}$La(2)N(4)	140.6(2)

Note: *Symmetry transformations used to generate equivalent atoms: $^{\#1}$ $-x, -y+1, -z+2$; $^{\#2}$ $-x+1, -y+1, -z+1$.

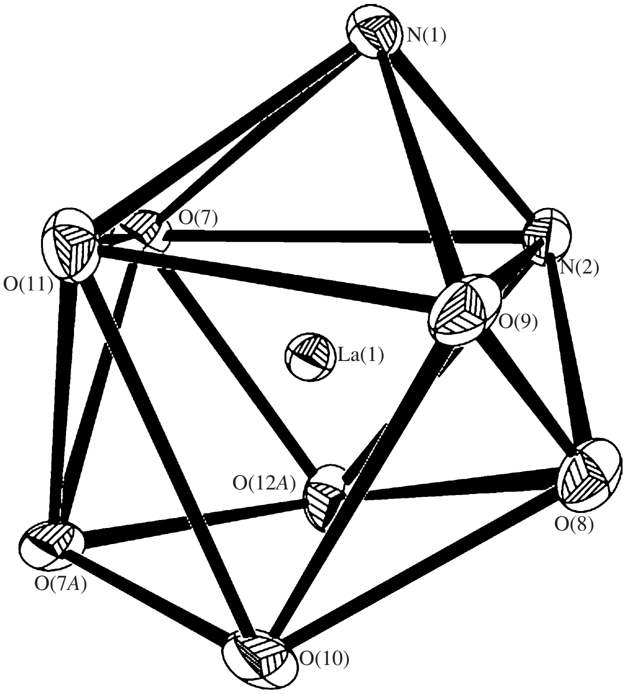

Fig. 2. Coordination polyhedron of the La^{3+} ion in complex **I**, La(1).

These complexes show similar stepwise thermal decomposition processes (Table 4). The thermal decomposition process of $La_2(o\text{-MBA})_6(Phen)_2 \cdot H_2O$ (**I**) can be divided into four steps as follows:

$$La_2(o\text{-MBA})_6(Phen)_2 \cdot H_2O \longrightarrow La_2(o\text{-MBA})_6(Phen)_2 \longrightarrow La_2(o\text{-MBA})_6 \longrightarrow La_2(COO)_2 \longrightarrow La_2O_3$$

The thermal decomposition processes of complexes **II**–**IV** are similar to complex **I**, which may be expressed by the following schemes:

$$Pr(o\text{-MBA})_3Phen \longrightarrow Pr(o\text{-MBA})_3 \longrightarrow 1/6\ Pr_6O_{11},$$

$$Y(o\text{-MBA})_3Phen \longrightarrow Y(o\text{-MBA})_3 \longrightarrow 1/2\ Y_2O_3,$$

$$Yb(o\text{-MBA})_3Phen \longrightarrow Yb(o\text{-MBA})_3 \longrightarrow 1/2\ Yb_2O_3.$$

Table 4. Decompostion temperature range of the complexes **I**–**IV***

Complex	T_l	T_s	T_m	T_f
I	107–220	263–400	400–568	568–744
II		201–397		397–621
III		156–386		386–681
IV		188–400		400–596

Note: **l* – lost solvent molecular, *s* – start, *m* – middle, *f* – final.

Based on the above thermal decomposition processes, the Phen is degraded from the complex firstly, this can be explained by the fact that the Ln–N bond lengths are less stable and easy to be broken down by the crystal data of La^{3+} [22]. From the data of Table 4, one can conclude that these complexes exhibit fine stablity to heating.

The antibacterial activity results, expressed as the diameter of the growth inhibition area in millimeters, are given in Table 5. One can conclude the following: (1) rare-earths chloride or *o*-MBA exhibited poor antimicrobial activities against *E. coli* and *S. aureus*; (2) Phen and their complexes expressed similar antibacterial activity against *E. coli* and*S. aureus*; (3) the antibacterial activity of these complexes will increase along with the rise of their concentration in the range of tested concentrations. The antimicrobial mechanism is presumably that the compounds have a good lipophilic nature arising from chelation [23]. The action mode of antimicrobials may involve different targets in pathogens, e.g., interference with cell wall synthesis and damage to the cytoplasmic membrane, as a result of which cell permeability may be altered leading to cell death [24].

Thus, ternary rare-earth complexes (Ln = La, Pr, Y, Yb) with *o*-methylbenzoic acid and 1,10-Phenanthroline have been synthesized and structurally characterized. According to the antibacterial testing results, these complexes expressed active antibacterial activitiy against *E. coli* and *S. aureus*.

Table 5. Inhibition zone diameter of the compounds (mm) (*Escherichia coli*/*Staphylococcus aureus*)

Compound	$c \times 10^{-3}$, mol/l				
	4.00	6.00	8.00	10.00	12.00
$LaCl_3 \cdot 6H_2O$	7.0/7.0	7.0/8.0	8.0/8.0	8.0/9.0	9.0/10.0
$PrCl_3 \cdot 6H_2O$	7.0/5.0	7.6/9.2	8.7/11.1	9.5/11.8	9.4/11.9
$YCl_3 \cdot 6H_2O$	7.0/5.0	6.0/8.9	8.3/11.3	8.5/6.0	8.8/11.2
$YbCl_3 \cdot 6H_2O$	5.4/10.2	7.4/9.9	7.0/9.0	9.4/9.6	8.8/11.2
o-MBA	6.0/6.0	6.0/6.0	6.0/6.0	6.0/6.0	6.0/7.0
Phen	11.0/14.0	12.5/14.70	16.0/18.0	17.5/19.0	19.0/21.0
$La_2(o\text{-MBA})_6(\text{Phen})_2 \cdot H_2O$	12/8.3	13.7/11.0	15.0/13.3	17.7/15.0	19.7/19.0
$Pr(o\text{-MBA})_3(\text{Phen})$	10.4/6.5	12.7/10.0	15.9/15.5	17.5/17.5	18.6/19.8
$Y(o\text{-MBA})_3(\text{Phen})$	13.2/8.9	14.6/10.0	16.2/12.5	17.4/15.9	21.0/17.6
$Yb(o\text{-MBA})_3(\text{Phen})$	13.2/10.2	15.1/12.2	17.60/17.3	18.3/19.3	20.1/21.6

ACKNOWLEDGMENTS

This work was supported by National Natural Science Foundation of China (no. 20773034), the Natural Science Foundation of Hebei Province (no. B2007000237), Hebei Education Department (no. 2006125) and Hebei Normal University (L2005B17), P. R. China.

REFERENCES

1. Wang, B.D., Yang, Z.Y., and Li, T.R., *Bioorgan. Med. Chem.*, 2006, vol. 14, p. 6012.
2. Li, T.R., Yang, Z.Y., Wang, B.D., et al., *Eur. J. Med. Chem.*, 2008, vol. 43, p. 1688.
3. Deng, R.W. and Zhang, Z.S., *Rare Earths*, 1987, no. 3, p. 36.
4. Picard, C., Geum, N., Nasso, I., et al., *Bioorg. Med. Chem. Lett.*, 2006, vol. 16, p. 5309.
5. Fricker, S., *Chem. Soc. Rev.*, 2006, vol. 35, p. 524.
6. Hemmila, I. and Mukkala, V. M., *Crit. Rev. Clin. Lab. Sci.,* 2001, vol. 38, p. 441.
7. Pandya, S., Yu, J.H., and Parker, D., *Dalton Trans.*, 2006, p. 2757.
8. Regulacio, M.D., Pablico, M.H., Vasquez, J.A., et al., *Inorg. Chem.*, 2008, vol. 47, p. 1512.
9. Supkowski R.M., Bolender J.P., Smith W.D., et al., *Coord. Chem. Rev.*, 1999, vol. 185–186, p. 307.
10. Aime, S., Geninatti Crich, S., Gianolio, E., et al., *Coord. Chem. Rev*, 2006, vol. 250, p. 1562.
11. He, Q.Z., Yang, J., Min, H., et al., *Mater. Lett.*, 2006, vol. 60, p. 317.
12. Fan, Y.H., He, X.T., Bi, C.F., et al., *Russ. J. Coord. Chem.*, 2007, vol. 33. no. 7, p. 535.
13. Ravi, K., Amresh K., Chandrashekar, and Anil Kumar, K. S., *Phosphorus Sulfur*, 2008, vol. 183, p. 1410.
14. Sheldrick, G.M., *SHELXS-97*, *Program for the Solution of Crystal Structure*, Göttingen (Germany): Univ. of Göttingen, 1997.
15. Sheldrick, G.M., *SHELXL-97*, *Program for the Refinement of Crystal Structure*, Göttingen (Germany): Univ. of Göttingen, 1997.
16. Zhang, Y.L., Liu, W.S., Wei, D., et al., *Spectrochim. Acta, A.*, 2004, vol. 60, p. 1707.
17. Yang, Y.T. and Zhang, S.Y., *Spectrosc. Lett.*, 2004, vol. 37, no. 1, p. 1.
18. Yan, B., Zhang, H.J., Wang, S.B., et al., *J. Photoch. Photobio., A*, 1998, vol. 112, p. 231.
19. Yu, H., He, Q.Z., Yang, J., et al., *J. Rare-Earth.*, 2006, vol. 24, no. 4, p. 4.
20. Nakamoto, K., *Infrared and Raman Spectra of Inorganic and Coordination Compounds*, New York: John Wiley & Sons, 1986, p. 239.
21. Li, J.Z., Li, G., and Yu, W.J., *J. Rare-Earth.*, 2000, vol. 18, no. 3, p. 233.
22. Zhang, J.J., Xu, S.L., Ren, N., et al., *Russ. J. Coord. Chem.*, 2007, vol. 33, no. 8, p. 611.
23. Chaudhary, A., Dave, S., Saini, R.K., et al., *Main Group Met. Chem*, 2001, vol. 24, p. 217.
24. Chaudhary, A., Bansal, N., Gajraj, A., et al., *J. Inorg. Biochem.*, 2003, vol. 96, p. 39.